doi:10.1246/cl.2010.994

Published on the web August 7, 2010

Fabrication and Enhanced Rectifying Performance of $Zn_{1-x}Co_xO$ Nanowall Vertically Growing on Si Wafer

Guoxing Zhu,[1] Yuanjun Liu,[2] Chi Zhang,[1] Zonglong Zhu,[1] and Zheng Xu*[1]
[1]*State Key Laboratory of Coordination Chemistry, School of Chemistry and Chemical Engineering, Nanjing University, Nanjing 210093, P. R. China*
[2]*Department of Materials Science and Engineering, Nanjing University, Nanjing 210093, P. R. China*

(Received May 6, 2010; CL-100429; E-mail: zhengxu@nju.edu.cn)

Mesocrystalline ZnO and Co-doped ZnO nanowall/p-Si heterojunctions are prepared by a chemical precursor route, which exhibits a rectifying behavior with a lower turn-on voltage tuned by Co^{2+} dopant concentration.

ZnO has attracted extensive interests in the research of wide band gap optoelectronic devices such as light-emitting diodes, laser diodes, and detectors due to its direct wide band gap (ca. 3.37 eV) and high exciton binding energy (ca. 60 meV) at room temperature.[1] For the application of ZnO-based optoelectronic devices, it would be highly preferred to make well-ordered ZnO nanowires or nanowalls aligned on cheap and CMOS (complementary metal oxide semiconductor) compatible substrate like silicon forming heterojunction.[2,3] However, heterojunction devices show a lower efficiency than homojunction devices, because the energy barrier formed at the junction interface decreases carrier injection efficiency, especially for heterojunctions with large band offset.[4] Tuning the heterointerface to nanoscale can increase the carrier injection efficiency, although it is still a challenge.[4,5] In addition, doping is a useful method to tune the semiconductor parameter, such as the energy band, and will improve the performance of heterojunction.

Owing to these reason, herein, hierarchical ZnO and Co-doped ZnO nanowall arrays were grown on single-crystal silicon plate (p-type) forming heterojunction nanostructures by a simple chemical solution route. Cobalt was selected as a dopant because of its excellent capability of decreasing the band gap.[6] The heterojunction shows a well-defined and enhanced rectifying behavior.

In our experiment (detailed sample preparations are given in Supporting Information (SI)[7]), hierarchical ZnO and Co-doped ZnO nanowall arrays were prepared via the precursor, zinc carbonate hydroxide hydrate (ZCHH) (SI-1 and SI-2) followed by thermal decomposition.[7] The XRD patterns of the obtained $Zn_{1-x}Co_xO$ ($x = 0$, 0.007, and 0.014) nanowalls are attributed to hexagonal ZnO phase (SI-3). The shift of XRD diffraction peaks evidences the dopant ions into the lattice (SI-3). The actual doping concentrations were determined by inductively coupled plasma quantometer and gives similar values ($Zn_{0.992}Co_{0.008}O$ and $Zn_{0.984}Co_{0.016}O$, respectively) to calculation values upon the ratio of the starting materials.

Thermal decomposition of the metal carbonate hydroxide compounds generates metal oxides without morphological deformation.[8] The typical scanning electron microscopy (SEM) image of the obtained ZnO product shown in Figure 1a shows that ZnO retains initial structure of nanowalls. This suggests that ZnO/substrate heterostructures can be easily obtained by this precursor route. Compared with the reported

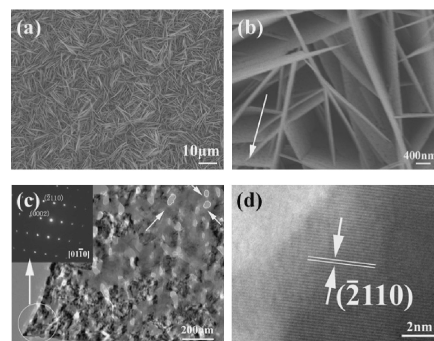

Figure 1. a, b) SEM and c, d) TEM images of ZnO nanowalls prepared by annealing from the ZCHH precursors, the arrows show the pore in the wall. The inset is the corresponding electron diffraction pattern.

methods[2,9] for construction of n-type ZnO/p-type substrate heterostructures such as plasma-assisted deposition, molecular beam epitaxy growth, etc., this route consumes little energy and requires no complicated hardware. The high-magnification SEM image (Figure 1b) and transmission electron microscopy (TEM) image (Figure 1c) show the porous features of the nanowalls. The selected area electron diffraction (SAED) pattern recorded on the area noted by a circle shows a sharp diffraction dot array, which is the feature of a single crystal, and can be attributed to (01$\bar{1}$0) lattice plane. The feature of single crystal is also concluded from the SAED patterns on other areas or a whole wall. The high-resolution TEM image (Figure 1d) recorded at the edge of the nanosheet indicated by a circle in Figure 1c exhibits clear lattice fringe corresponding to ($\bar{2}$110) crystal plane. All of these clearly show that the nanowall is a mesocrystal,[10] which exhibits the same diffraction feature as that of single crystal but the shape and structure is completely different from the classical single crystal. The cobalt-doped ZnO nanowalls have similar shape and mesocrystal structure features with undoped ZnO (SI-4 and SI-5).[7] The uniform distribution of cobalt atoms is concluded from the EDS spectra (SI-4).

Electron transport measurements of the as-prepared $Zn_{1-x}Co_xO$ nanowall/Si heterojunctions were carried out by two electrodes stuck on both sides of the sample with silver paste. The current–voltage (I–V) characteristic curves of the heterojunction at room temperature in air are shown in Figure 2a, exhibiting a nonlinear, well-defined rectifying behavior. It shows the enhanced rectifying behavior by cobalt doping. A ln plot of I versus V of Figure 2a is shown in Figure 2b. According to the I–V characteristics of the real diodes,[11]

© 2010 The Chemical Society of Japan

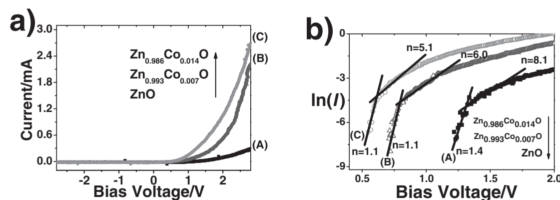

Figure 2. a) The I–V characteristics of the $Zn_{1-x}Co_xO$ nanowall/Si heterojunctions and b) a ln plot of current versus bias voltage of a) with (A) $x = 0$, (B) 0.007, and (C) 0.014.

$$I = I_o[\exp(V/(nV_t)) - 1] \quad (1)$$

$$n = (q/kT)(dV/d\ln(I)) \quad (2)$$

where k is the Boltzmann constant, T is the absolute temperature, and n is the junction ideality factor, which is determined from the slope of the straight line region of the forward bias $\ln(I)$–V characteristics through eq 2. According to the equation and Figure 2b, the value of n for the ZnO/Si heterojunction is about 1.4 when the forward bias is 1.2–1.3 V, and about 8.1 when the forward bias is 1.3–1.6 V. While n for the $Zn_{0.993}Co_{0.007}O$/Si heterojunction is about 1.1 when the forward bias is 0.7–0.8 V and about 6.0 when the forward bias is 0.8–1.2 V, and that of $Zn_{0.986}Co_{0.014}O$/Si heterojunction is about 1.1 when the forward bias is 0.5–0.6 V and about 5.1 when the forward bias is 0.6–0.9 V.

According to the Sah–Noyce–Shockley theory, the value of the ideality factor in a p–n junction is 1.0 at a low voltage and 2.0 at a higher voltage.[11,12] However, the theory model cannot account for ideality factors greater than 2.0 found here. This may result from the presence of nonlinear metal–semiconductor contact in the system.[11] As the case of diamond/ZnO p–n heterojunction reported by Yang and co-workers,[11] the basal heterojunction diode can be modeled by a series of diodes or resistances in a dissimilar bias voltage range: the actual p-Si/n-ZnO heterojunction diode, Ag/p-Si Schottky diode (or contact resistance), and Ag/n-ZnO Schottky diode (or contact resistance). In the low bias voltage range, the device can be modeled by a combination of a heterojunction and two resistances, which is in good agreement with the experiment ($n = 1.1$), where as in the interim bias voltage range, a group of these diodes is usually used to model the various conduction mechniasms.[11,13] When the diode voltage is $V_i \gg kT/q$ and only considering the linear region of the $\ln(I)$ vs. V characteristic, the ideality factor can be considered as the sum of the ideality factor of the individual rectifying junction. Accordingly, it is apparent that the ideality factor of the real diode $\gg 2$ can be measured. In the high bias voltage range, I–V plot is linear, which can be modeled by a group of three resistances. The p–n heterojunction fabricated here is stable, and the rectifying performance remains unchanged in a period of three months at least.

Generally speaking, the substitution of Co into ZnO (Co_{Zn}) should not contribute donor or acceptor characteristics since the outer shell of Co is isoelectronic with Zn. But in this case, the influence of the electrons in the hypo-outer shell of Co should be taken into account. The hypo-outer shell of Co is the d states which generally appear near the Fermi level.[14] Co^{2+} locates at the center of the tetrahedron made of four oxygen atoms. The d states of Co split into a higher energy triplet state and a lower double state under the influence of the tetrahedral crystal field to form high-spin Co^{2+} with fully filled e state and half-filled t_2 state. The former participates in valence band, while the later one hybridizes with the p orbital of the valence band and further splitting into the bonding states and antibonding states. The bonding states participate in the bonding (Co–O) and are hence localized. However, the antibonding states have a higher energy level and are very close to the conduction band, and the electrons in this state have a higher probability of jumping to the conduction band, resulting in the increase of conductivity with the increase of Co concentration in ZnO. Also, such s–d and p–d exchange interactions give rise to a negative and a positive correction to the conduction and the valence band edges, respectively, leading to a band gap narrowing,[15] which cause the decrease of the turn-on voltage of p–n junction semiconductor diode.[16]

In conclusion, we presented a chemical precursor route to fabricate vertical mesocrystalline ZnO and Co-doped ZnO nanowall arrays on cheap and CMOS compatible p-Si plate. The obtained n-$Zn_{1-x}Co_xO$ nanowall/p-Si heterojunction exhibits a well-defined and reliable rectifying behavior with a lower turn-on voltage tuned by Co^{2+} dopant concentration. The realization of n-type $Zn_{1-x}Co_xO$ nanowall/p-type Si heterojunction will open up opportunities for low-cost and high-performance optoelectronic devices based on these nanostructure arrays. The character of mesocrystalline Co-doped ZnO with bigger surface area is of advantage for the heterojunction application in the sensor field.

Financial support from National Basic Research program (973 program 2007CB936302) and the National Natural Science Foundation of China under major project No. 90606005 is greatly appreciated.

References and Notes

1 For example: M. E. Fragalà, A. D. Mauro, G. Litrico, F. Grassia, G. Malandrino, G. Foti, *CrystEngComm* **2009**, *11*, 2770.
2 H. Zhu, C.-X. Shan, B. Yao, B.-H. Li, J.-Y. Zhang, D.-X. Zhao, D.-Z. Shen, X.-W. Fan, *J. Phys. Chem. C* **2008**, *112*, 20546.
3 C.-H. Chao, W.-H. Lin, C.-H. Chen, C.-H. Changjean, C.-C. Pan, C.-F. Lin, *Chem. Lett.* **2010**, *39*, 202.
4 X. Duan, Y. Huang, R. Agarwal, C. M. Lieber, *Nature* **2003**, *421*, 241.
5 C.-F. Pan, J. Zhu, *J. Mater. Chem.* **2009**, *19*, 869.
6 S. V. Bhat, F. L. Deepak, *Solid State Commun.* **2005**, *135*, 345.
7 Supporting Information is available electronically on the CSJ-Journal Web site, http://www.csj.jp/journals/chem-lett/index.html.
8 E. Hosono, S. Fujihara, I. Honma, H. S. Zhou, *J. Mater. Chem.* **2005**, *15*, 1938.
9 H. Ohta, M. Hirano, K. Nakahara, H. Maruta, T. Tanabe, M. Kamiya, T. Kamiya, H. Hosono, *Appl. Phys. Lett.* **2003**, *83*, 1029.
10 F. C. Meldrum, H. Cölfen, *Chem. Rev.* **2008**, *108*, 4332.
11 C.-X. Wang, G.-W. Yang, H.-W. Liu, Y.-H. Han, J.-F. Luo, C.-X. Gao, G.-T. Zou, *Appl. Phys. Lett.* **2004**, *84*, 2427.
12 C. Sah, R. N. Noyce, W. Shockley, *Proc. IRE* **1957**, *45*, 1228.
13 J. C. Ranuárez, F. J. G. Sánchez, A. Ortiz-Conde, *Solid-State Electron.* **1999**, *43*, 2129.
14 D.-W. Wu, Z.-B. Huang, G.-F. Yin, Y.-D. Yao, X.-M. Liao, D. Han, X. Huang, J.-W. Gu, *CrystEngComm* **2010**, *12*, 192.
15 K. J. Kim, Y. R. Park, *Appl. Phys. Lett.* **2002**, *81*, 1420.
16 K. Huang, R. Han, *Semiconductor Physics*, Chinese Science Publishing House, Beijing, **1979**, p. 119.

 © 2010 The Chemical Society of Japan